CHAPTER IV

RESULTS

1. The Effect of Gamma Irradiation on *A. annua* Plantlets

The dose-survival curve of gamma irradiation on *A. annua* plantlets showed that the radiation dose of 8 Gray (Gy) gave 50 % survival of the plantlets with variable artemisinin content. Figure 15 shows the percent survival of *A. annua* plantlets in various doses of gamma irradiation and Figure 16 shows the characters of the obtained irradiated plantlets. It can be seen that at the dose of γ-ray below 5 Gy, the plantlets showed more leaves, stems, roots than the plantlets obtained from the 8 Gy treatment. The 8-Gy dose plantlets also showed some leaf abnormalities which might affect the efficiency of subsequent *ex vitro* transfer to the field. Figure 17 shows the appearance the plantlets that were irradiated with the doses of 5 and 8 Gy. Therefore, in this study, the gamma dose of 5 Gy was used for the shoot-tip irradiation. Under this treatment, the plantlets showed almost 70 % survival with mostly in good morphological appearance. We have shown that 90 samples of the *in vitro* plantlets obtained from this dose contain artemisinin in a wide range from 0.02 to 0.67 % dry weight, with less than 10 % of the plantlets containing artemisinin more than 0.5 % dry weight (Figure 18) (Koobkokkruad *et al.*, 2007).

Subsequently, some *in vitro* plantlets obtained from the previous studies were transferred to *ex vitro*. It should be noted that the irradiated shoots could be cultured and regenerated to complete plantlets with long shoots with roots on normal MS medium without adding plant growth regulators. Figure 19 shows some plantlets that

were cultured on MS medium containing 3 % sugar and 0.8 % agar. The plantlets were kept in 40 $\mu mol.m^{-2}.s^{-1}$of fluorescence light for 6 week-olds. The plantlets showed blight green leaves with more thinness and fully expanding than those the control leaves. It was observed that some of the irradiated plants were more dark greenish and smaller than the control leaves and had no root differentiation in each treatment. (variant 5) (Figure 19).

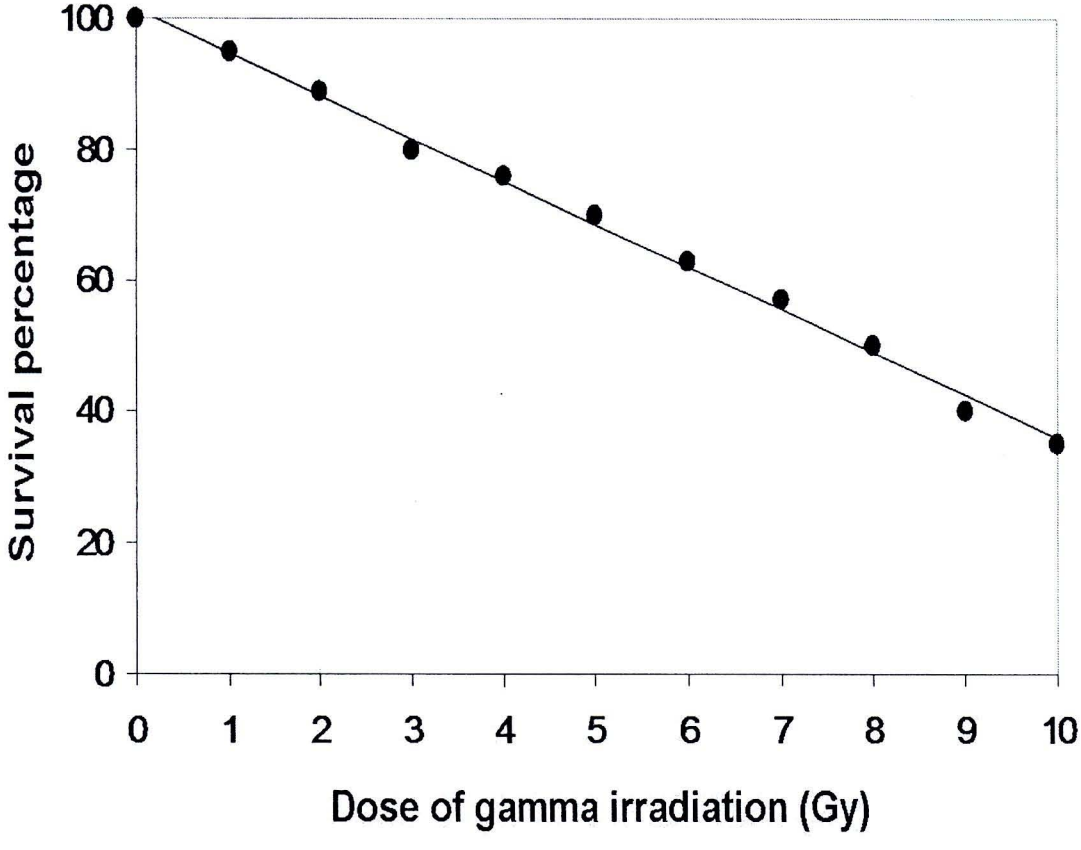

Figure 15 Effect of low-dose of gamma irradiation on the survival percentage of *in vitro* plantlets of *A. annua*

Figure 16 *A.annua* plantlets developed from shoots tips that had been treated with gamma irradiation with various doses of 0, 3, 5, 8 and 10 Gy and cultured *in vitro* for 4 weeks

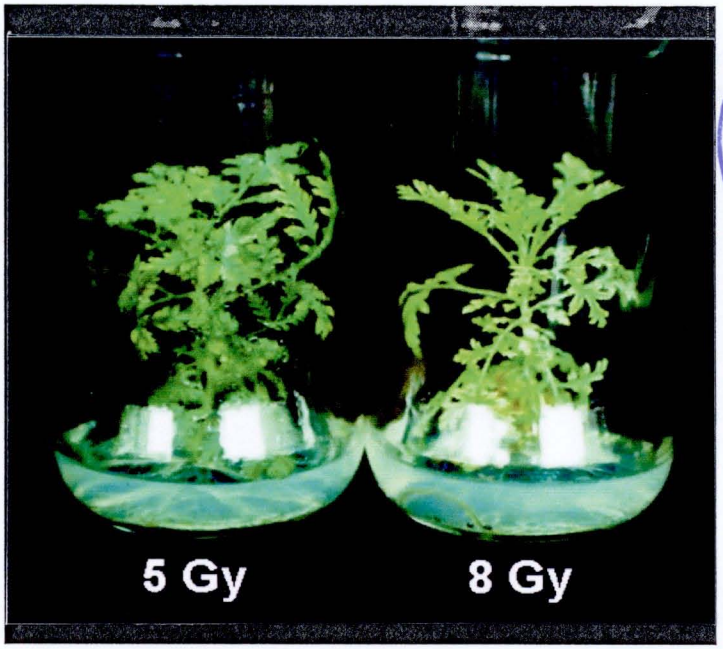

Figure 17 *A.annua* plantlets that had been irradiated with 5 and 8 Gy of γ-rays and cultured *in vitro* for 4 weeks

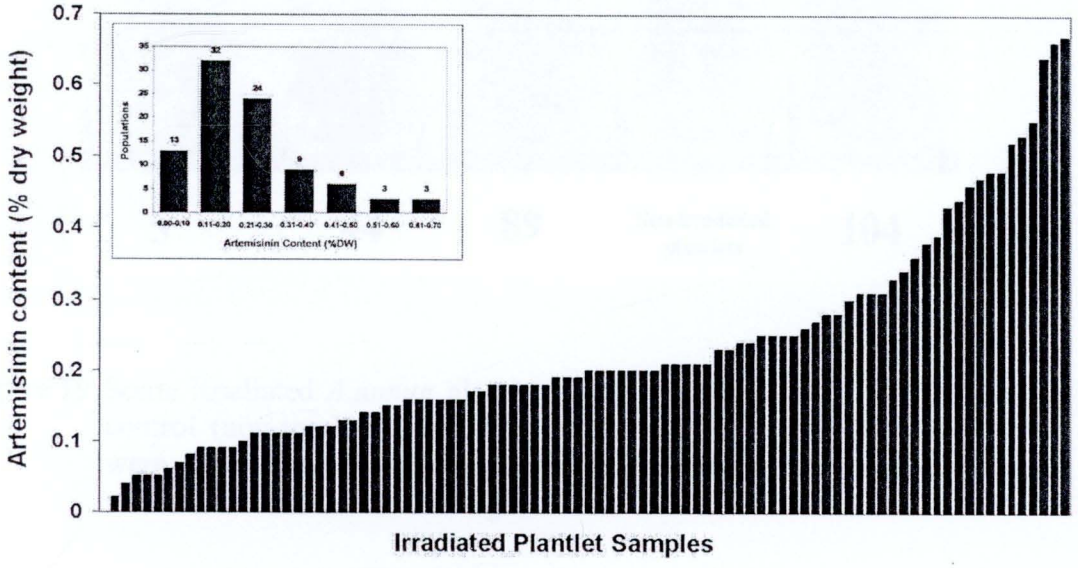

Figure 18 Variation of artemisinin content in various plantlets of *A. annua* that their shoot tips that had been exposed to a dose of 5 Gy of gamma rays. Inset shows distribution of the plantlet samples in various range of artemisinin content (Koobkokkruad *et al.*, 2007)

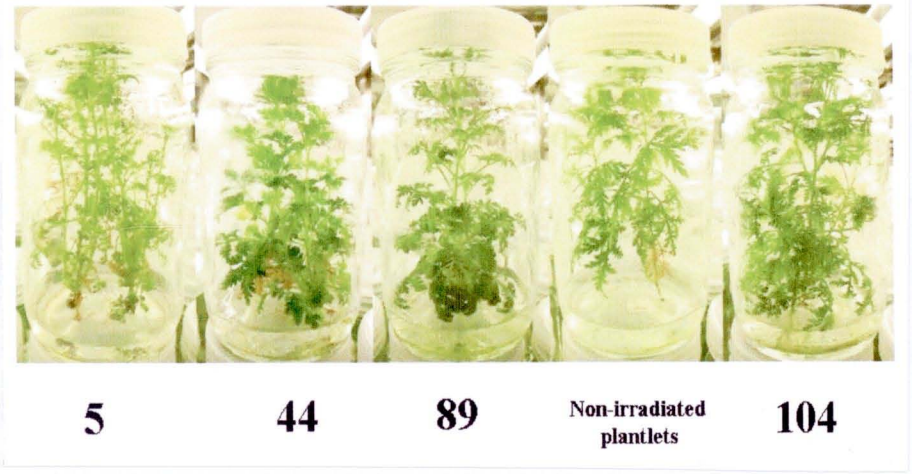

Figure 19 Some irradiated *A.annua* plantlets of the samples no. 5, 44, 89, 104 and control (non-irradiated plantlets) in Figure 18. These *in vitro* plantlets were grown on MS medium containing 3 % sugar and 0.8 % agar. in 40 $\mu mol.m^{-2}.s^{-1}$ of fluorescence light

Figure 20 The appearance of the leaves of the gamma irradiated *A.annua* plantlets (sample number 86, 104 and 218) compared with the leaf of the non-irradiated plantlets

2. The Transfer of *In vitro* Plantlets to *Ex vitro* Conditions for Plant Growth and Development of *A. annua*

The acclimation of *in vitro A. annua* plantlets was studied for effective transfer of *A. annua* of the *in vitro* irradiated plantlets to the *ex vitro* conditions (the green house and open field). The plantlets were subcultured on MS medium containing 3 % sugar and 0.8 % agar and kept in 40 $\mu mol.m^{-2}.s^{-1}$of fluorescence light for 6 week-olds. Each plantlet with complete shoot and root was selected to transfer to the acclimation conditions (Figure 21, a). The root of each selected plantlets was first cleaned to remove of agar medium with steriled water, and transferred to a bottle (16-oz) containing 50 ml liquid hormone-free MS medium (without sugar) with 50 ml vermiculite as medium absorbent. All the transferred plantlets were kept in 40 $\mu mol.m^{-2}.s^{-1}$of fluorescence light for 8 week-olds. A piece of membrane filter was attached over a hole of each plastic cap for increasing air exchange of the culture vessel (Figure 21, b). When the shoot of each plantlet was fully grown in the bottle, the plastic cap was losen for 1 week until the shoot grew to the top of the bottle. Then, the plastic cap was removed for another 1 week (Figure 21, c). After that, the plant was transferred to 4-inch pot with steriled soil and incubated for 15 days at 25±1 $^{\circ}C$ under 40 $\mu mol.m^{-2}.s^{-1}$ photosynthetic photon flux density provided by cool-white fluorescence lamps (Figure 21, d-f) that the irradiated plants (with 5 Gy) grow normally during the process of *in vitro* and *ex vitro* transfer. The plants were then transferred to grown *ex vitro* in a green house of Chulalongkorn University, Bangkok and some were transferred to grow in the open field (30-38/20-29 $^{\circ}C$, day/night, air temperature) at Kanchanaburi Province, Thailand for a total period of 10 months (January-October 05).

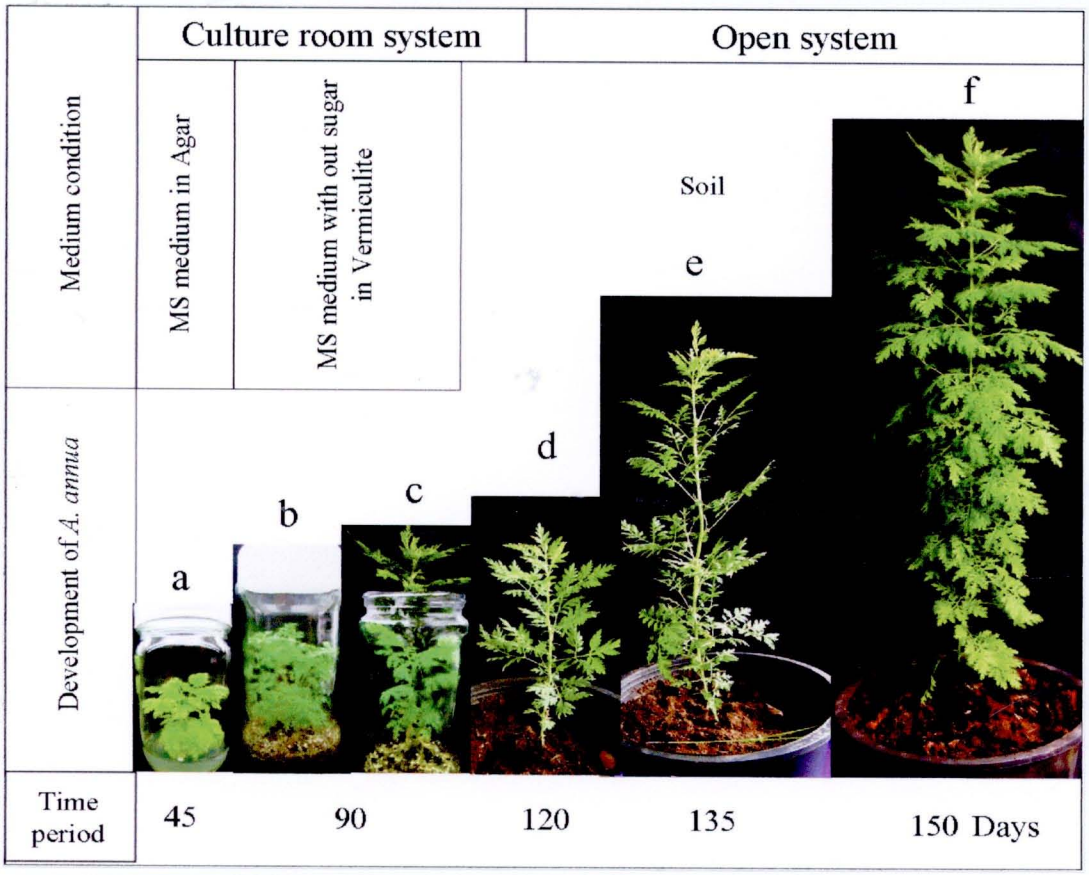

Figure 21 A summary of the process from *in vitro* plantlets (a-d) to the *ex vitro* conditions (e-f) of *A. annua*

3 Analysis of Artemisinin Content in *In vitro* Plantlets and *Ex vitro* Plants of *A. annua*

Plants were harvested and determined for their artemisinin content by the TLC-densitometric method described previously (Koobkokkruad, et al., 2007). Figure 22 shows TLC-densitometric chromatograms of hexane extracts prepared from some leaf samples of the irradiated plantlets. It can be seen that the peak of artemisinin in each sample was well detected and separated from other constituents present in the crude extracts. The peak showed symmetrical shape with very low baseline noise. Based on the TLC-densitometric method, it was found that the content of artemisinin in selected 23 samples of the *in vitro* irradiated plantlets appeared to be highly variable in a wide range from 0.09 to 0.69 % of dry weight (DW) (Figure 23).

For the *in vitro-ex vitro* transfer to the green house, it was found that the *in vitro* plantlets contained artemisinin content in range of 0.06 to 0.66 % DW (mean = 0.30) and the *ex vitro* plants in the green house contained in the range of 0.12 to 0.42 % DW (mean = 0.27) (Figure 24). Interestingly, data analysis of the artemisinin content between the *in vitro* plantlets and the *ex vitro* plants in green house appeared to be highly correlated ($r = 0.956^{**}$, $p = 0.01$) (Figure 25).

For the open field samples, the artemisinin content of that *in vitro* plantlets to *in vitro* plants was in the range of 0.25 to 0.69 % DW (mean = 0.40), compared with the *ex vitro* plantlets which were found to be in the range of 0.31 to 0.84 % DW (mean = 0.43) (Figure 26). Again, the data analysis of the artemisinin content between the *in vitro* plantlets and the *ex vitro* plants in open field also showed highly correlated ($r = 0.814^{**}$, $p = 0.01$) (Figure 27).

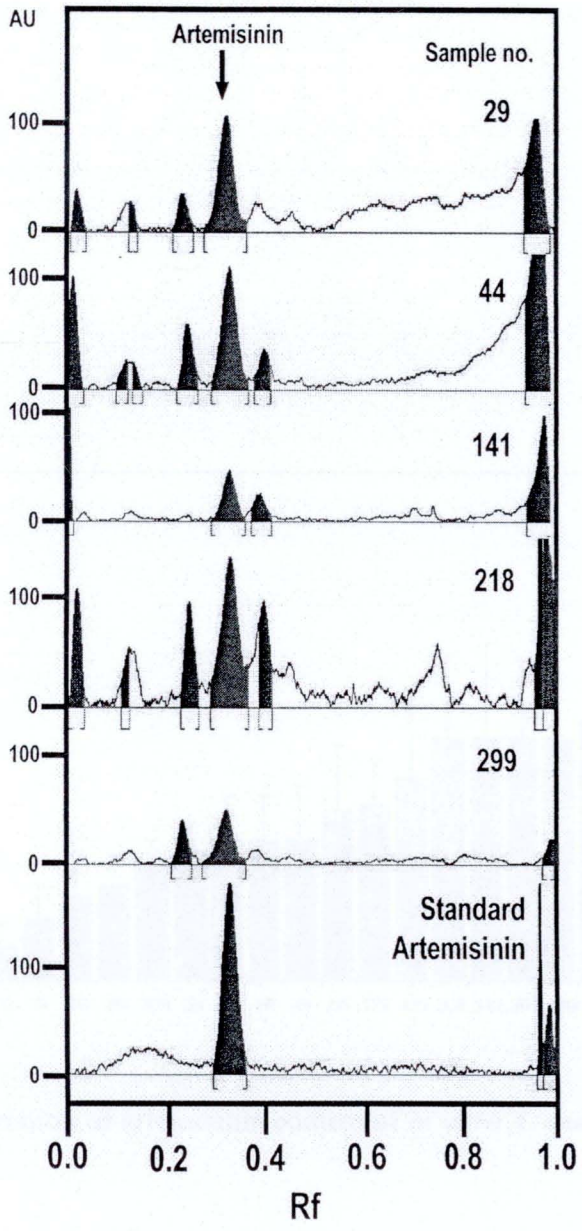

Figure 22 TLC chromatograms of *A. annua* at the some gamma irradiated

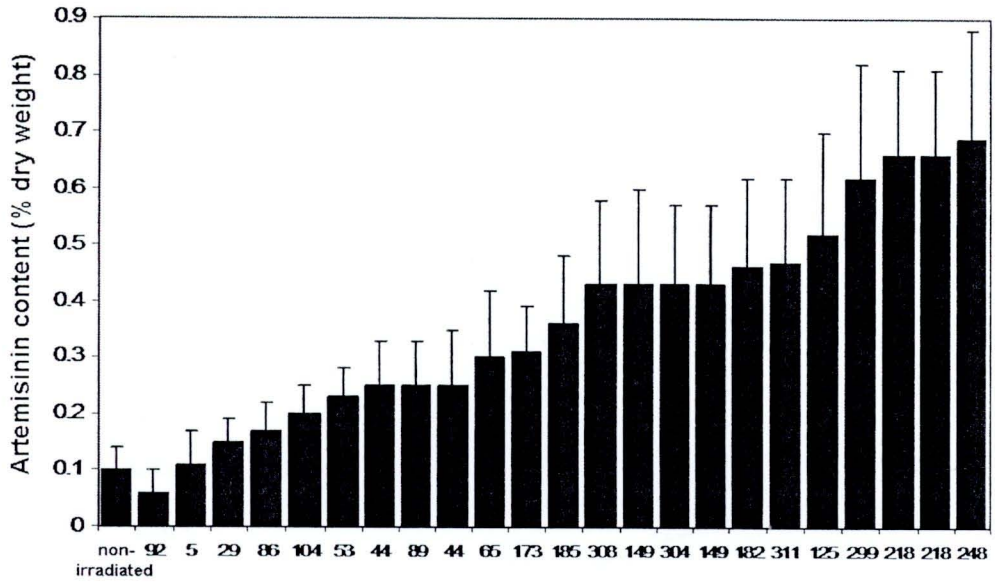

Figure 23 Variation of artemisinin content of *in vitro A. annua* plantlets

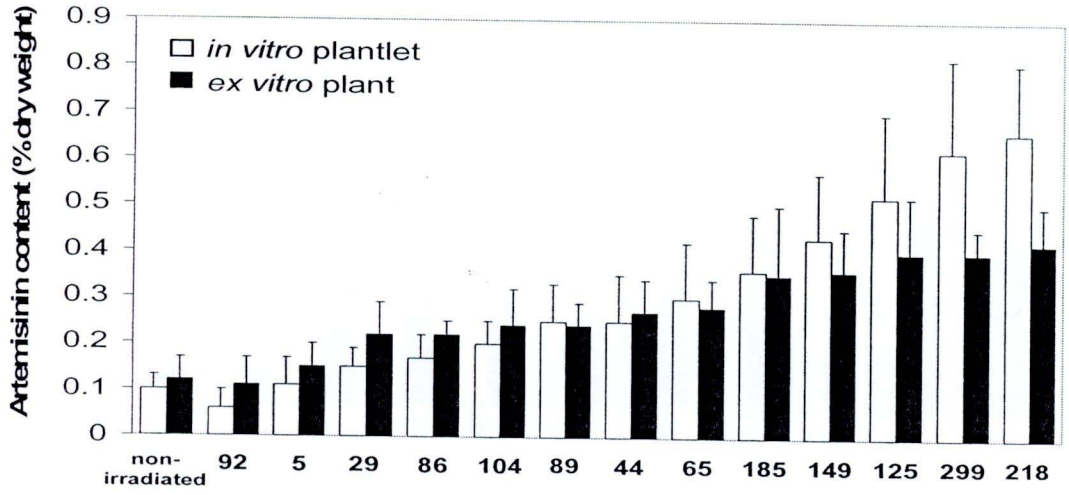

Figure 24 Comparison of artemisinin content of *in vitro A. annua* plantlets (□) and *ex vitro* plant in greenhouse (■)

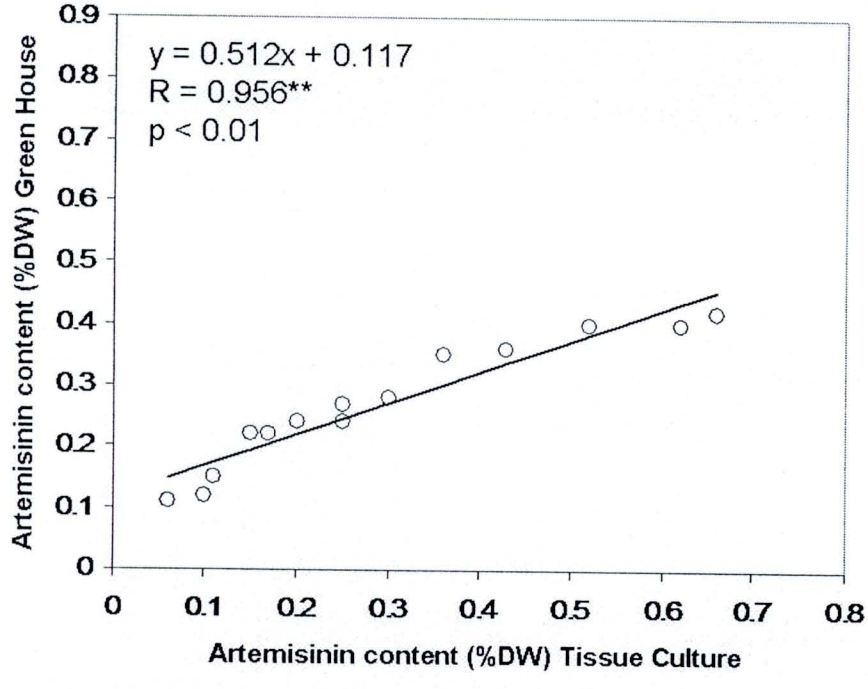

Figure 25 Correlation curve of artemisinin content between the *in vitro* plantlets and *ex vitro* plant in greenhouse of irradiated *A. annua*

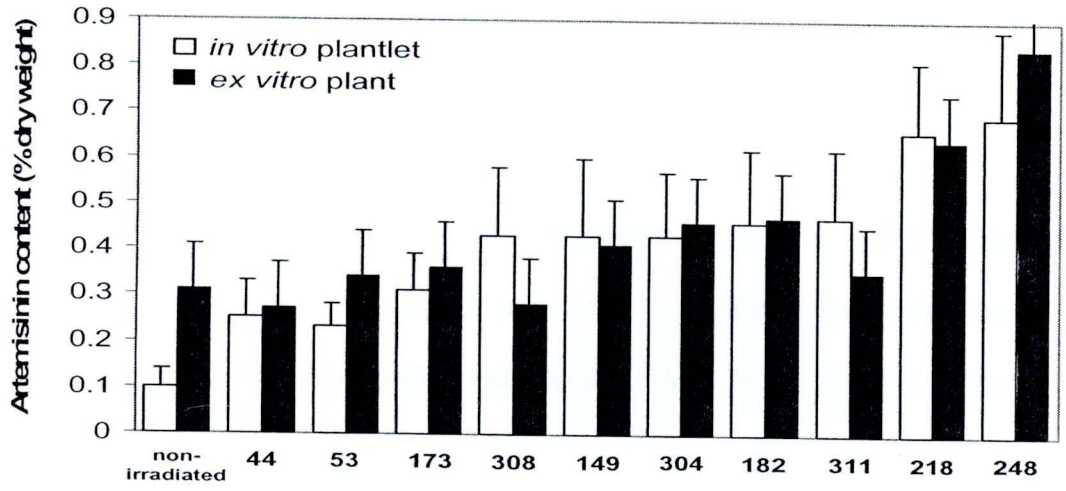

Figure 26 Comparison of artemisinin content of *in vitro A. annua* plantlets (□) and *ex vitro* plant in open-field (■)

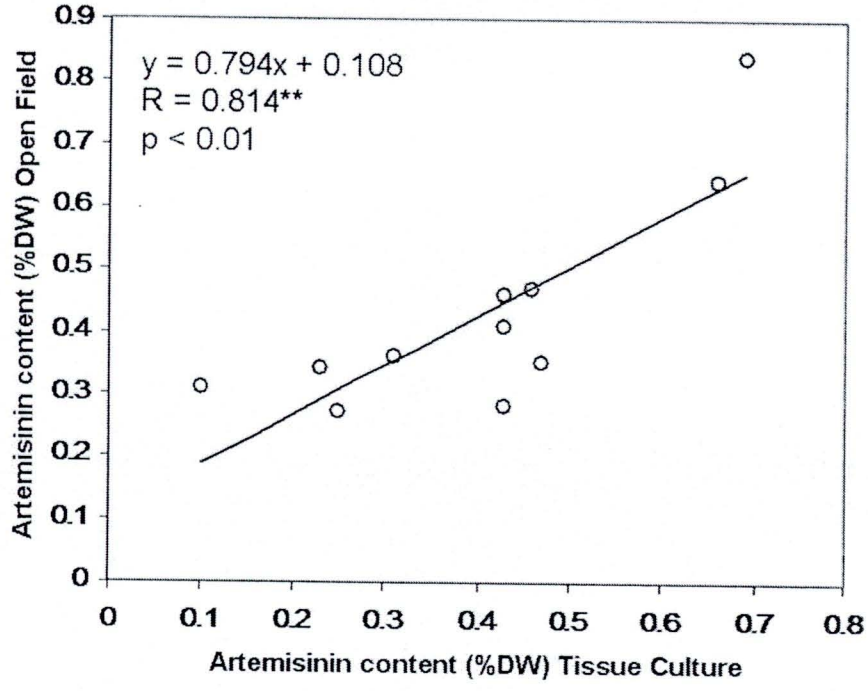

Figure 27 Correlation curve of artemisinin content between the *in vitro* plantlets and *ex vitro* plant in open-field of irradiated *A. annua*

4. Cloning and Expression of *Amorpha-4,11-Diene Synthase* Gene in *A. annua* Plants

4.1 Construction and nucleotide sequence of amorpha-4,11-diene synthase

As described in the Materials and Methods, the full-length gene of amorpha-4,11-diene synthase was amplified from total RNA by RT-PCR. The PCR reaction mixture was performed with the template of the total RNA and the primer of sense and antisense. The specific primers were designed from GenBank that contained *ads* gene sequences from previously reported (Wallaart et al. 2001; Chang *et al.*, 2000; Merck *et al.*, 2000). The primers were sense *ads*1 (5'-CG GGATCC ATG TCA CTT ACA GAA G) and antisense *ads*2 (5'CGA CTCGAG TCA TAT ACT CAT AGG ATA AA), which included the restriction sites (underlined) for *Bam*H I and *Xho* I. After digestion with *Bam*H I and *Xho* I, the gene was ligated into pET24a(+) expression vector (Figure 28) in order to contain His-tag and T7-taq at the N-terminus. The ligated products were then transformed into competent cells of *E. coli* strain BL21 and screened on LB agar plate containing kanamycin. The single colony of the kanamycin resistance was confirmed the plasmid transformation by PCR specific for *ads* gene. Figure 29 shows the PCR product of *ads* gene in the kanamycin resistance strain. Subsequently, the corresponding pET24a(+) plasmid was used for determining of the DNA sequence.

By DNA sequencing, it was found that the chimerical *ads* gene was 1,638 nucleotides. The deduced amino acid sequence of open reading frame was 546 amino acids (Figure 30).

The alignments of deduced amino acid sequence of ADS were performed. The ADS amino acid sequences were download from GenBank included AY006482

(Wallaart et al. 2001), AJ251751 (Change et al., 2000), DQ241826 (unpublished), EF197888 (unpublished) and AF138959 (Merck et al., 2000). It was found that the alignment scare between our ADS amino acid sequence were 98.53, 98.71, 97.80, 98.53 and 98.71, respectively. Figure 31 shows the alignment of ADS amino acid sequences from Genbank. These suggested that the chimeric gene was encoded for the amino acid sequence of ADS.

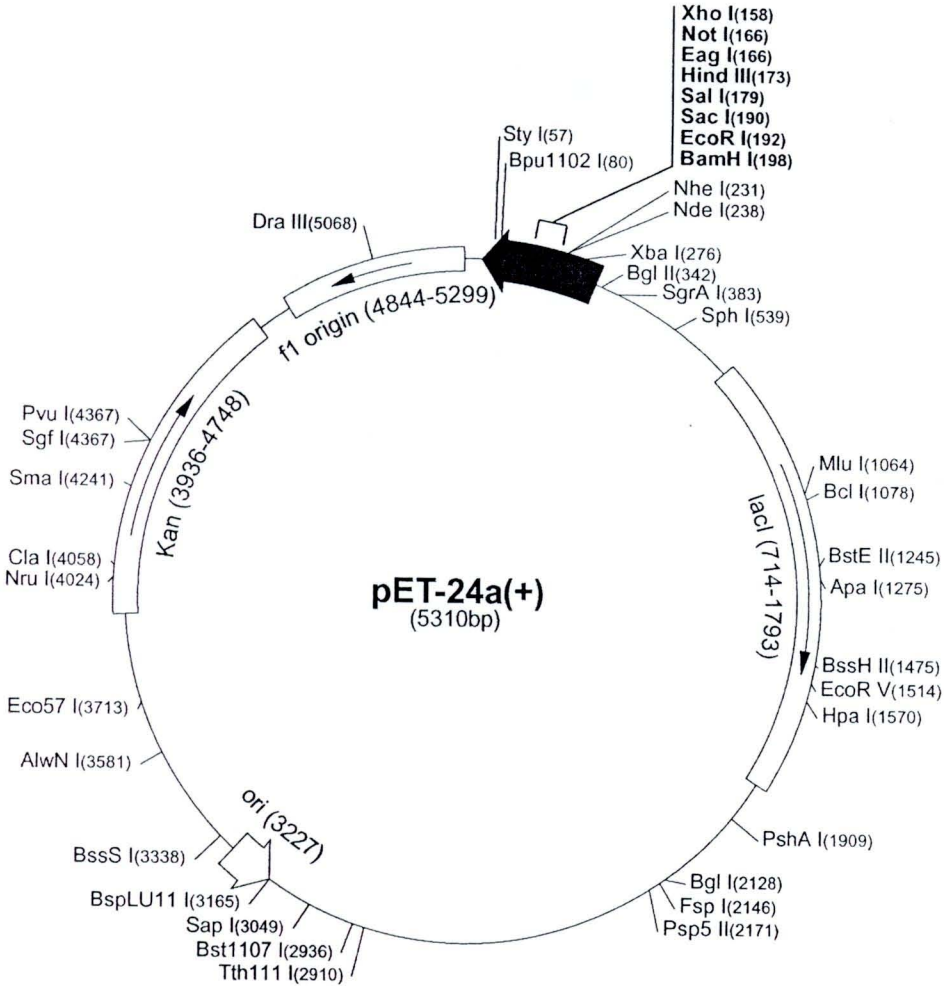

Figure 28 The pET-24a-d(+) vectors carry an N-terminal T7•Tag® sequence plus an optional C-terminal His•Tag® sequence.

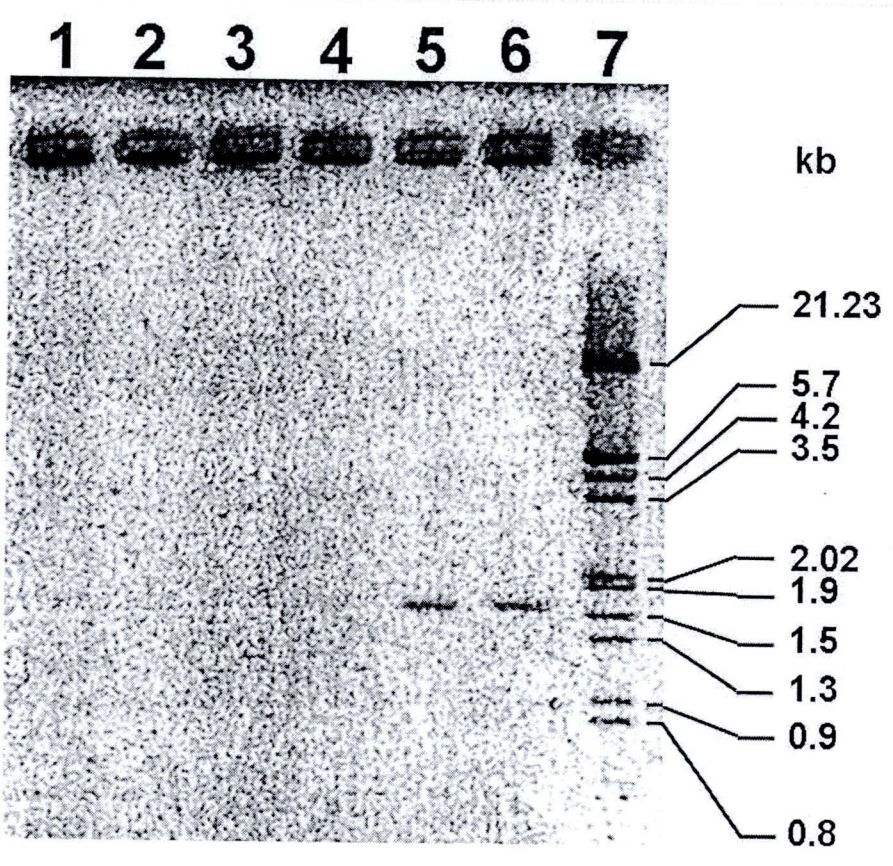

Figure 29 PCR analysis of *ads* gene inserted in pET24a(+) from various clones of *E. coli* BL21

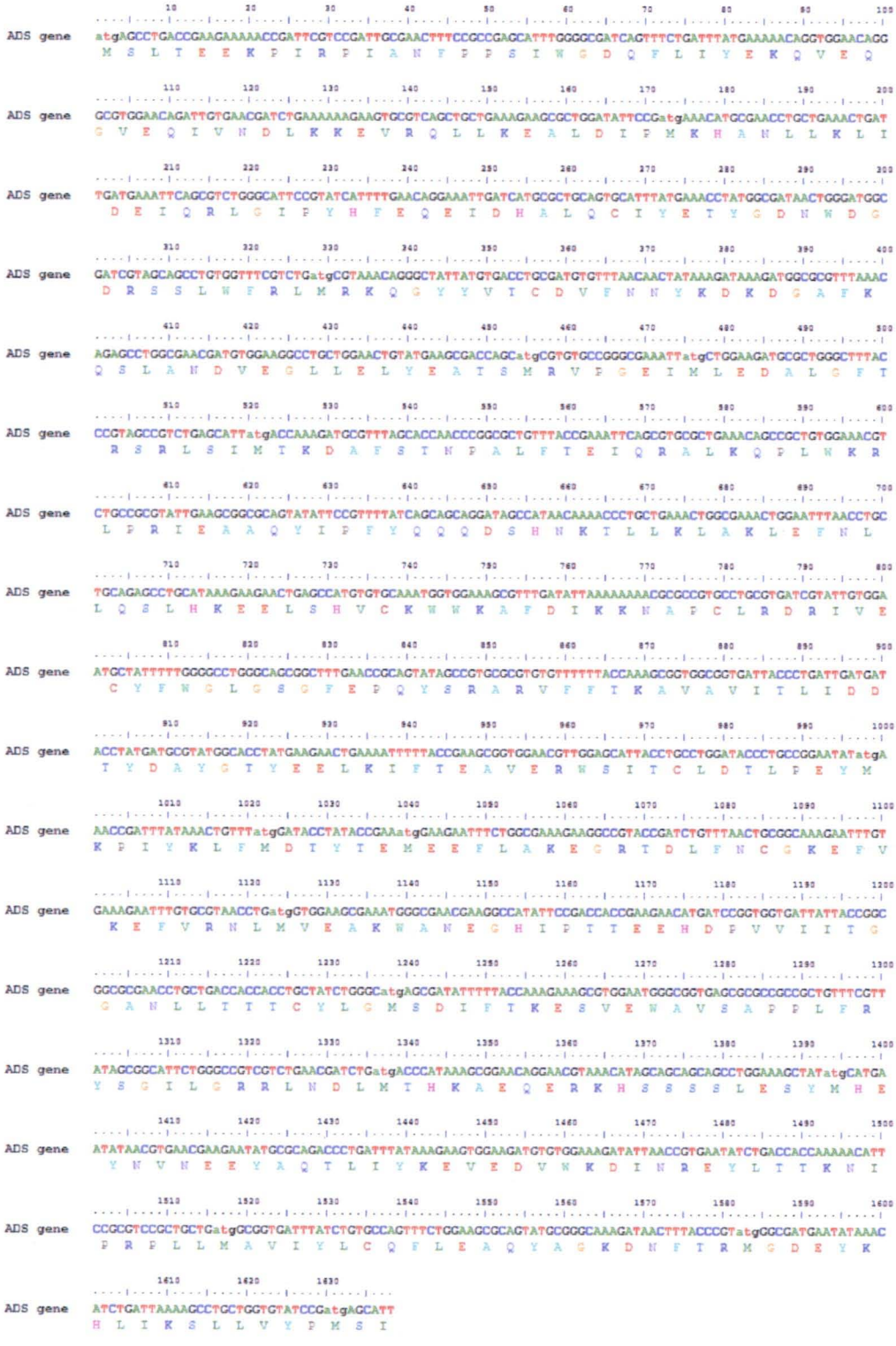

Figure 30 The full-length gene of *amorpha-4,11-diene synthase*

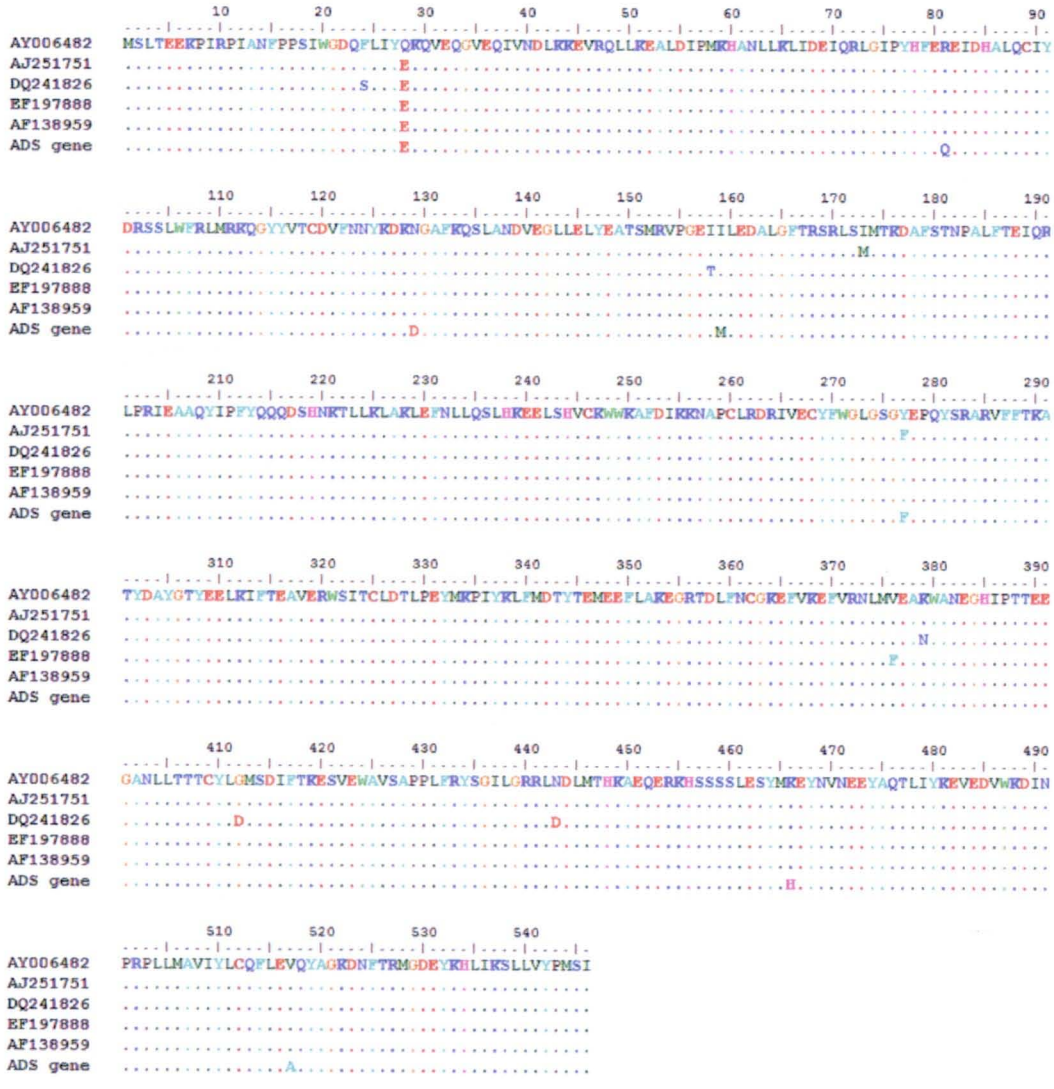

Figure 31 The alignment of amorpha-4,11-diene synthase from GenBank

4.2 The overexpression of *ads* gene in *E. coli*

ADS protein expression in *E. coli* was induced by IPTG. The ADS protein was extracted by 0.5 % Triton-X 100 buffer for 2 form of soluble and insoluble (inclusion body). The level of protein expression was determined by SDS-PAGE. It was found that the protein expression of ADS enzyme at accepted size of 56 kDa. Figure 32 shows the level of protein expression of ADS protein of soluble fraction up to 240 min (Figure 32A). The obtained protein band intensity showed that the protein expression was increased from continuously 30 to 120 min after the IPTG induction (Figure 32B). After that, there was no increase in the protein expression. However, most of the expression protein was found in the inclusion body (Figure 33). Therefore, the *ads* gene from *A. annua* was cloned and expressed successfully in *E. coli*.

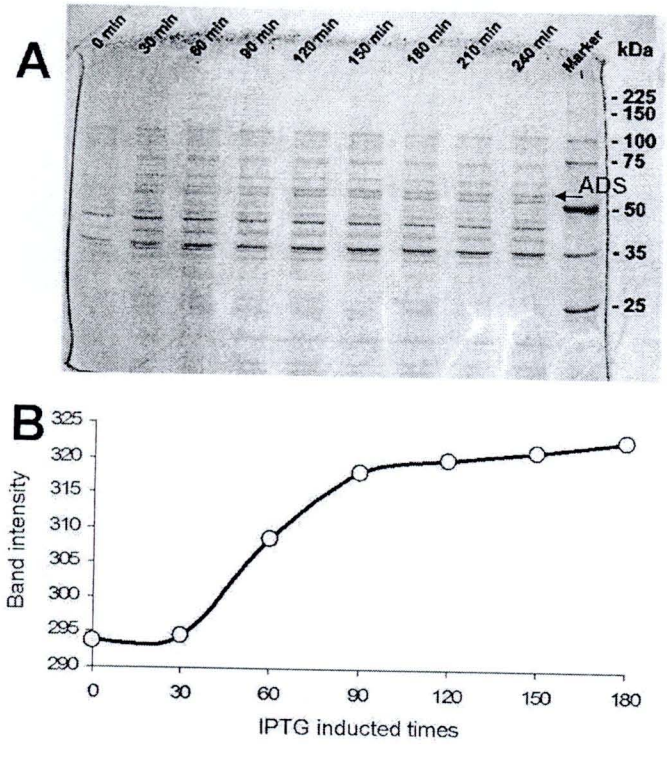

Figure 32 The SDS-PAGE pattern of soluble extract from positive clone of IPTG induced *E. coli* BL21 harboring pET24a(+)/*ads* in each times (A), Band intensity of ADS band in each time (B)

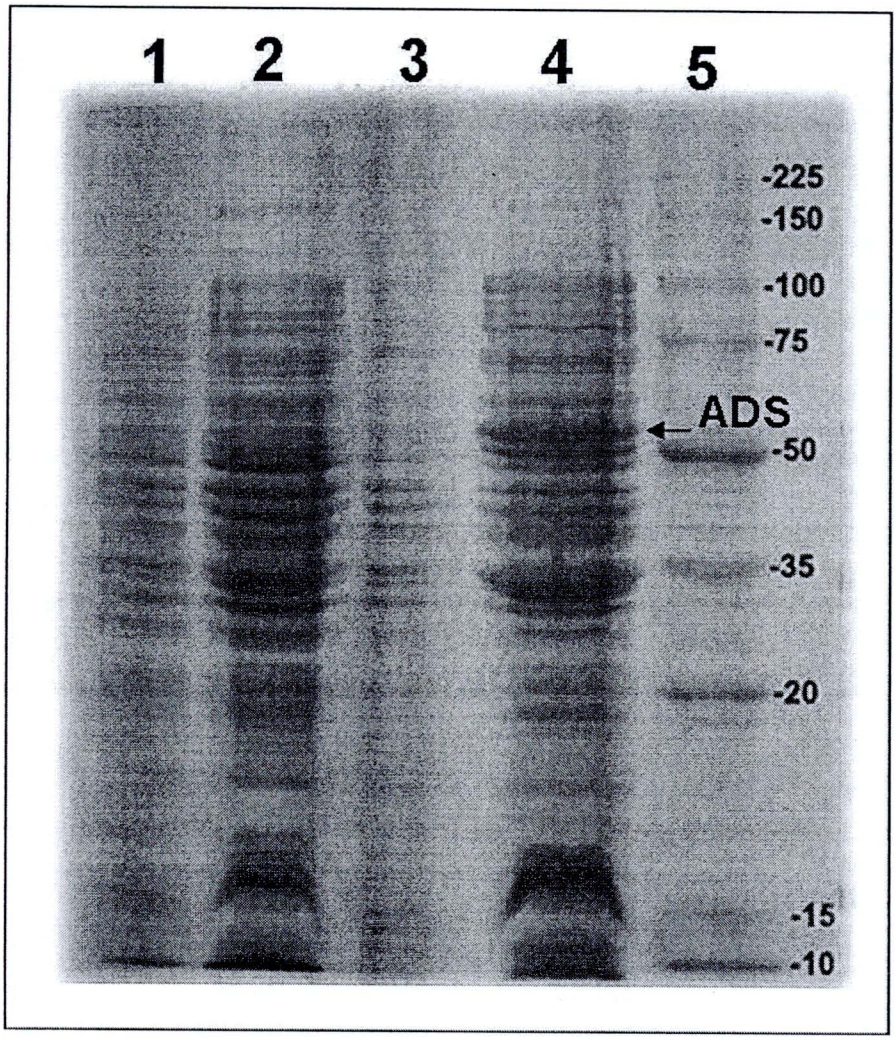

Figure 33 The comparison of SDS-PAGE pattern of soluble and insoluble protein extracted from positive clone of IPTG induced and non-IPTG induced *E. coli* BL21 harboring pET24a(+)/*ads* at 180 min

Lane 1 soluble fraction of non-IPTG induced clone
Lane 2 insoluble fraction of non-IPTG induced clone
Lane 3 soluble fraction of IPTG induced clone
Lane 4 insoluble fraction of IPTG induced clone
Lane 5 protein standard marker

4.3 Cloning of *ads* gene into plant expression vector pBI121

The *ads* gene from pET24a(+)/*ads* was subcloned between *Bam*H I and *Xho* I site into the plant expression vector pBI121. The plasmid pBI121/*ads* contained the CaMV 35s promoter/ chimeric *ads* gene and NOS terminator respectively and the NOS/NPTII gene for kanamycin resistance (Figure 34). The plant expression vector was then inserted into *A. tumefaciens* LBA4404 by triparental mating with the aid of the pRK 2013 helper plasmid. LB medium containing 25 mg/l kanamycin and rifampicin 50 mg/l were used to screen positive clones. The PCR with specific primers for *ads* gene was performed to confirm the vector transformation. The PCR product was electrophoresised by 0.5 % agarose gel. Figure 35 shows PCR product of the *ads* gene from the DNA template of positive control pBI121/*ads* (lane 1), *A. tumefeciencs* harboring pBI121/*ads* (lane 2) and DNA marker (lane 3). The PCR product was confirmed the *ads* gene at the size 1.6 kb. Consequently, *A. tumefeciencs* harboring inserted pBI121/*ads* was used as plant expression vector for *ads* gene transfer to *A. annua* through plasmid system.

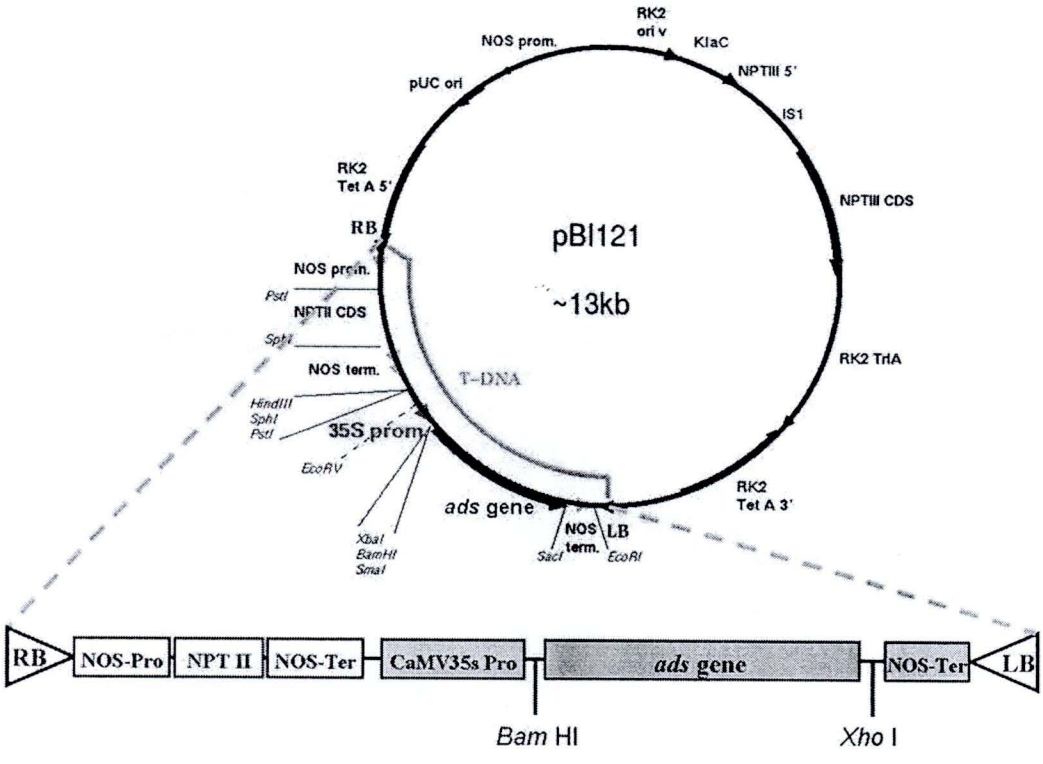

Figure 34 The plasmid construction of pBI121/*ads* containing CaMV 35s promoter/ chimeric *ads* gene and NOS terminator respectively and the *NOS/NPTII* gene for kanamycin resistance

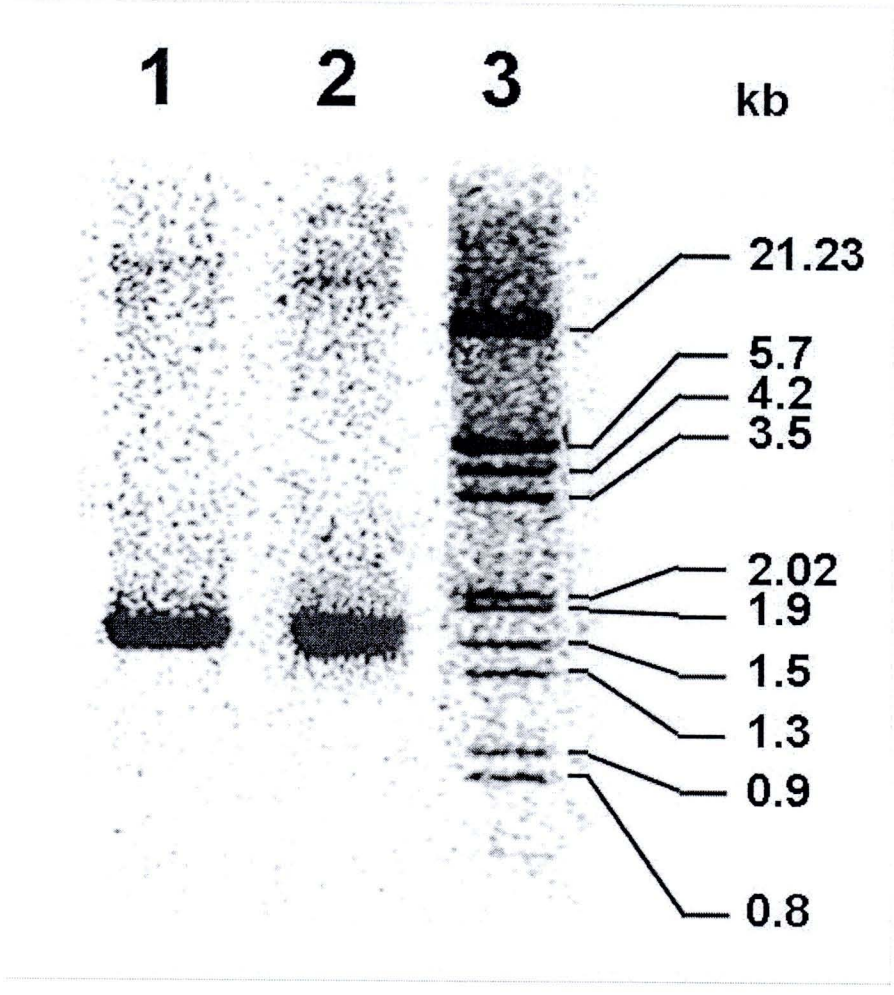

Figure 35 The PCR product of the *ads* gene from DNA template of purified pBI121/*ads* (Lane 1), *A. tumefeciencs* harboring pBI121/*ads* (Lane 2) and DNA markers (Lane 3).

4.4 *Agrobacterium*-mediated transformation of *ads* gene to *A. annua*

Shoot and stem explants of *A. annua* were infected with *A. tumefesiens* strain LBA4404 harboring the binary vector pBI121/*ads*. After two days, the explants were transformed onto the selective and regeneration medium as described in Materials and Methods. Figure 36 shows various steps of *Agrobacterium*-mediated transformation of *ads* gene to *A. annua*. The transformation medium was performed by using a

combination of selected medium and regenerated medium. Kanamycin was applied to the medium to select the kanamycin resistant shoots and inhibit growth of untransgenic *A. annua*. Based on the incorporation and expression of the *NPTII* gene during the selected steps, the selected medium was added with 10 mg/l kanamycine for each step of the transformation process. Subsequently, cefotaxime was added to inhibit *A. tumefaciens* growth. After being subcultured for one month in the selected medium, the explants were transferred to the second medium contained 300 mg/l cefotaxime and 10 mg/l kanamycine for one month. Then, the explants were transferred to the third medium containing 100 mg/l cefotaxime for another one month. Finally, the explants were transferred to the medium without the antibiotics. During the selected steps, *A. annua* explants were found to be quite sensitive to kanamycin and died after 1-2 months.

For the shoot regeneration, plant hormones were applied in each step of selected medium contained 0.1 mg/l TDZ. The survival explants were transformed to be calli at the scratched wound. Figure 37 shows that the calli were grown well on the regeneration medium. The morphological appearance of the transformed calli was yellow, bright green and dark green. The regenerated shoots were established after a calli formed the dark green pigment and more compactable. The results of *Agrobacterium*-mediated transformation of *ads* gene to *A. annua* was 20 clones of the regenerated shoots. When the regenerated shoots became 2-3 cm in length, they were transferred to a hormone-free MS medium for stimulation of roots and shoots elongation for 6 weeks. Subsequently, the shoots were micropropagated and then collected to determine for the presence of pBI121/*ads* transformation, the ADS enzyme activity and artemisinin content of the transgenic *A. annua*.

A. annua plantlet were grown on MS medium for 6 weeks

ads gene were inserted into *A. annua* by *A. tumefaciens*-mediated transferation.

2 days ↓ Incubated in dark room on MS medium

ads gene inserted in *A. annua* were regenerated on MS medium with 0.1mg/l TDZ, 10 mg/l kanamycine and 500 mg/l cefotaxime for 1 month

1 month ↓ 10 mg/l kanamycine and 300 mg/l cefotaxime

1 month ↓ 10 mg/l kanamycine and 100 mg/l cefotaxime

ads gene inserted in *A. annua* were regenerated on MS medium with 0.1mg/l TDZ, Non-antibiotic medium

Figure 36 The protocol of *Agrobacterium*-mediated transformation of *ads* gene to *A. annua*

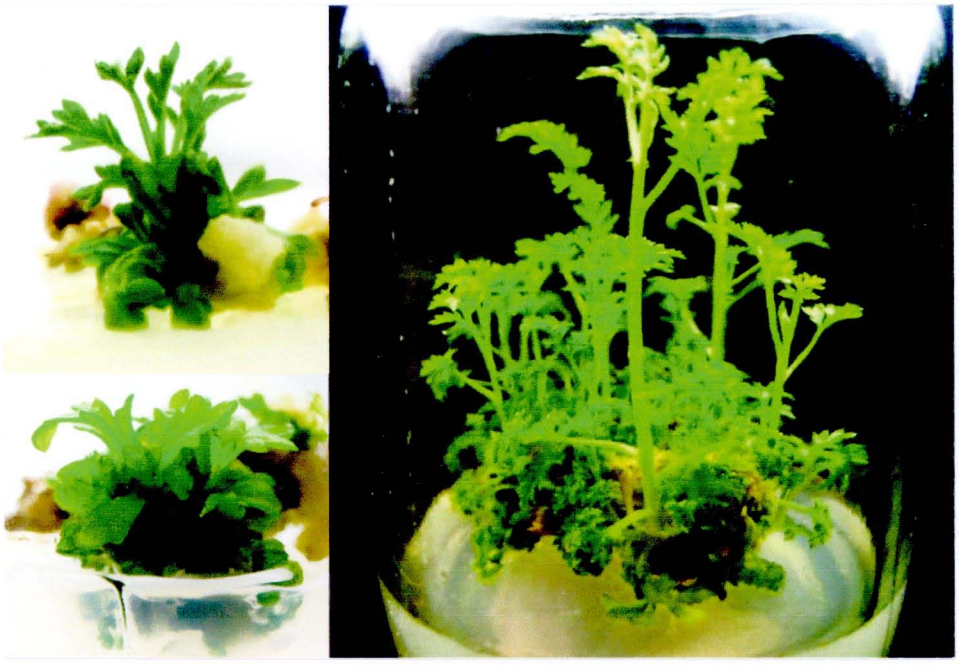

Figure 37 Regeration of *A. annua* on regeneration medium

4.5 PCR analysis of pBI121/*ads* in transformed *A. annua*

The transgenic plants detection was performed with putative transformants and wild-type of *A. annua* by PCR analysis. Genomic DNA was isolated from shoots of regenerated *A. annua*. The PCR analysis on the transgenic plants, using specific-primer for CaMV 35s promoter sequences, confirmed the integration of the chimeric cassettes of pBI121/*ads* into *A. annua* chromosomal genome. The PCR amplification of 20 regenerated clones were found the only one clone present the CaMV 35s promoter. Figure 38 demonstrated PCR product from DNA template of pBI121/*ads* as a positive control (lane 1), transgenic *A. annua* LBA4404 harboring pBI121/*ads* (lane 2), untransgenic *A. annua* and DNA marker (lane 4). The transgenic *A. annua* plants were amplified the CaMV 35s promoter at the size of 200 bp. The DNA sequence of PCR products were performed by BackMan DNA sequencing machine. The sequences alignment of the PCR product showed similar to CaMV 35s promoter E01311 in GenBank (Figure 39). These confirm the successes of *Agrobacterium*-mediated transformation of *ads* gene into *A. annua*.

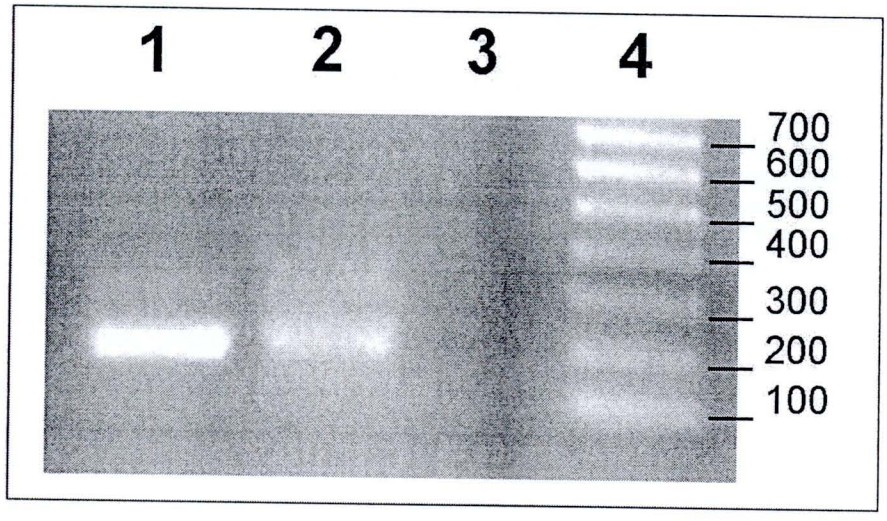

Figure 38 The PCR product from DNA template of pBI121/*ads* as a positive control (lane 1), transgenic *A. annua* LBA4404 harboring pBI121/*ads* (lane 2), untransgenic *A. annua* (lane 3) and DNA marker (lane 4).

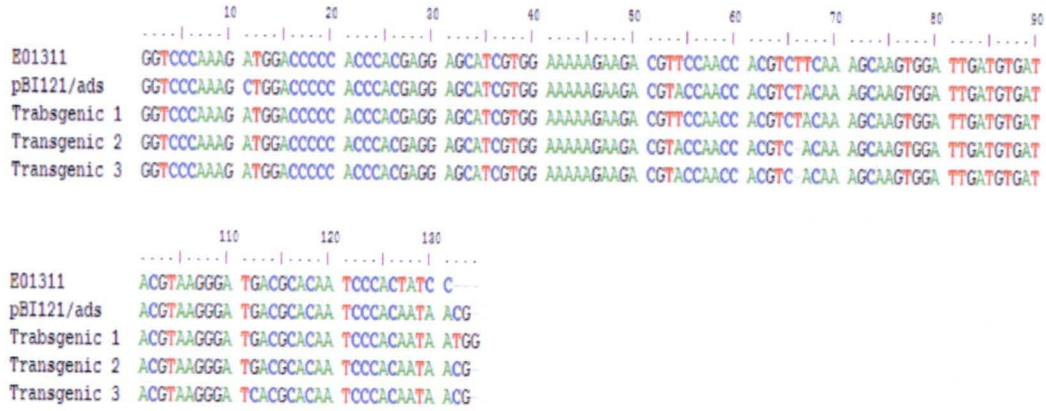

Figure 39 The alignment of CaMV 35s promoter DNA sequences (E01311) compared with sequences of amplified PCR product from DNA template of pBI121/*ads* as a positive control, transgenic *A. annua* LBA4404 harboring pBI121/*ads* in three reactions.

4.6 Amorpha-4,11-diene synthase assay in transgenic *A. annua*

As described in the Materials and Methods, an enzyme assay of amorpha-4,11-diene synthase has been reported previously by Bouwmeeteer *et al.,* (1999). Their method used radioactivity labeled [1-^{3}H(N)]FDP as substrate and detected the formation of the radioactive amorpha-4,11-diene by radiocounting using a liquid scientillation counter. In this study, the assay condition used in the reaction mixture was similar to that of Bouwmeesteer *et al.,* (1999), however, the step of the detection of radioactively labeled product was carried out by TLC-radioscan which detected directly the availability of the enzymatic product. In practice, the non-polar enzyme product of amorphar-4,11-diene was separated from the polar substrate by extracting the reaction mixture with 1 ml hexane. The hexane fraction was then evaporated to a small volume and spotted onto a silica gel plate. After that, the plate was developed under the solvent system of hexane : ethylacetate : acetic acid, 25:7:1 to separate the enzyme product from other compounds. The enzyme activity was then detected by TLC-radioscanner. Figure 40 shows typical TLC-radiochromatograms both of an enzyme-catalyzed reaction and a boiled control of an enzyme extract prepared from a untransgenic and transgenic *A. annua* plantlets. It can be seen that, the enzyme substrate of [1-^{3}H(N)] FDP did not appear in the TLC plate because of the polar property of the substrate which is not soluble in hexane while the enzyme product, amorpha-4,11-diene was detected clearly at the Rf value of 0.4. The boiled control that had no enzyme activity showed no conversion of [1-^{3}H(N)] FDP to the enzyme product.

The results of the enzyme activity were assayed in a reaction mixture used contained [1-^{3}H(N)]FDP (100,000 cpm) for 30 min in the similar protein concentration. This experiments were found to be similar to the activity from

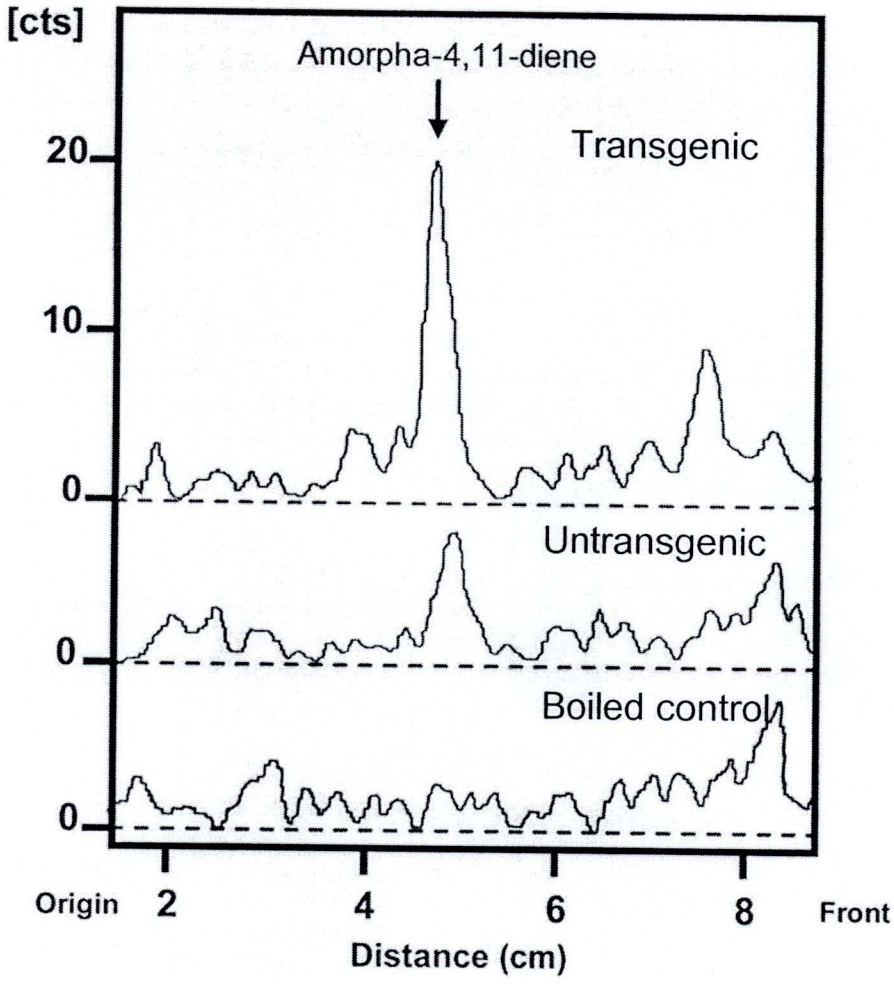

Figure 40 Typical TLC-radiochromatograms both of an enzyme-catalyzed reaction and a boiled control of an enzyme extract prepared from untransgenic and transgenic *A. annua* plantlets

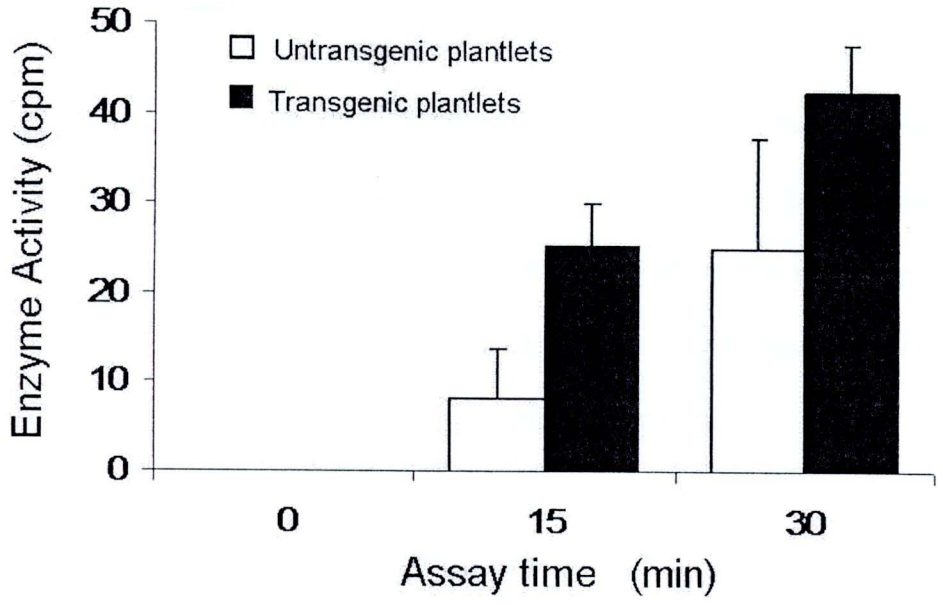

Figure 41 The relationship between ADS activity and assay time of the ADS enzyme-catalyzed reaction from untransgenic and transgenic *A. annua* plantlets

both of the transgenic and untransgenic *A. annua*. However, when cold FDP (non-labeled FDP) was added for ten folds of the hot [1-^{3}H(N)]FDP concentration in the assay reaction. During the assay time, the conversion of [1-^{3}H(N)]FDP to radioactive amorpha-4,11-diene was decreased by cold FDP. The clearly results of the enzyme assay was presented in Figure 41. The enzyme products were monitored at 0, 15 and 30 min assay time. The results showed the enzyme product in unit of cpm each point of the assay time. It was found that the amorpha-4,11-diene synthas activity from transgenic *A. annua* higher than untransgenic *A.annua* plant. The transgenic *A. annua* presented enzyme activity increased to two folds from untransgenic in each monitoring time. These results confirm that the CaMV 35s promoter induced the overexpression of ADS in transgenic *A. annua*. Consequently, the leaves of transgenic *A. annua* were collected for artemisinin analysis.

4.7 Artemisinin determination in transgenic *A. annua*

In terms of artemisinin analysis, the compound was detected by TLC-densitometric method (Koobkokkruad *et al.*, 2007). The leaves of *A. annua* harvested for 2 month after subcutured were dried in a hot air oven. The dried leaves from various samples of *A. annua* plantlets were ground and extracted under reflux. After cooling and precipitating of the extracted powder, the clear solution of crude extract was spotted directly (50 µl) onto a precoated silica gel (POLYGRAM^{R} SIL G/UV$_{254}$, 0.25 mm thinness, Merck, Germany) and developed by the solvent system of hexane:ethylacetate: acetone, 16 : 1 : 1. The TLC plate was then exposed with saturated ammonia at 100°C for 2 hours for chromophore development of artemisinin.

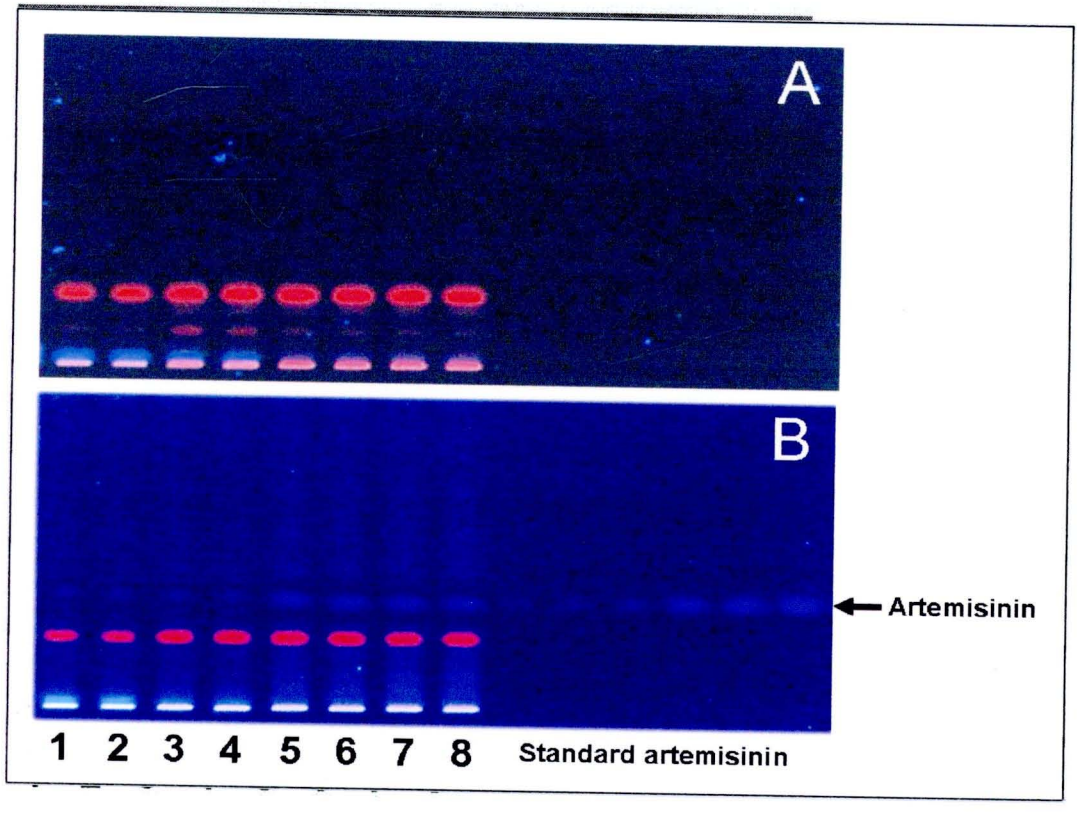

Figure 42 TLC patterns observed under UV 366 nm of some crude extracts prepared from the transgenic and untransgenic plantlets of *A. annua*. The position of artemisinin is indicated, before (A) and after (B) conversion of artemisinin to the chromophore compound
Lane 1-2 untransgenic plantlets
Lane 3-4 untransgenic plantlets collected from regeneration
Lane 5-8 transgenic plantlets

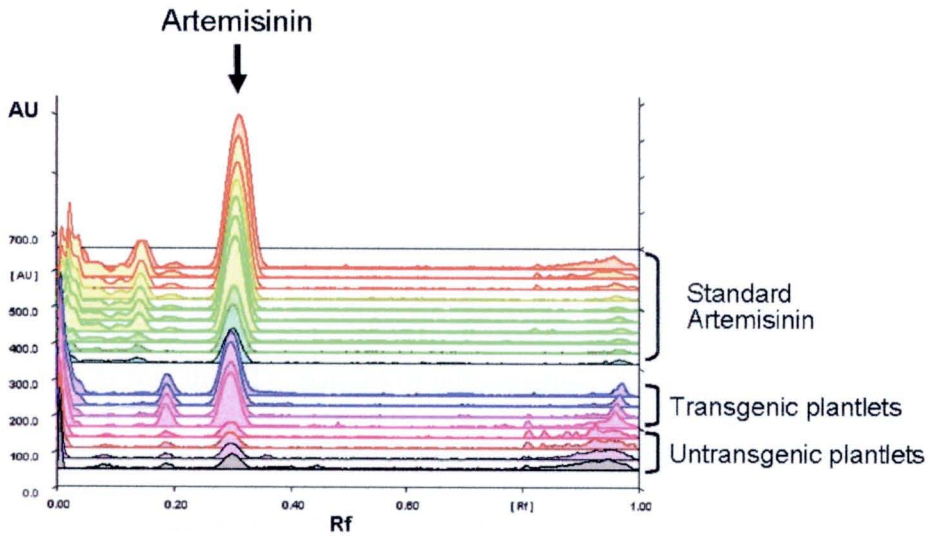

Figure 43 TLC chromatogram observed under UV 313 nm of crude extracts prepared from the transgenic and untransgenic plantlets of *A. annua*

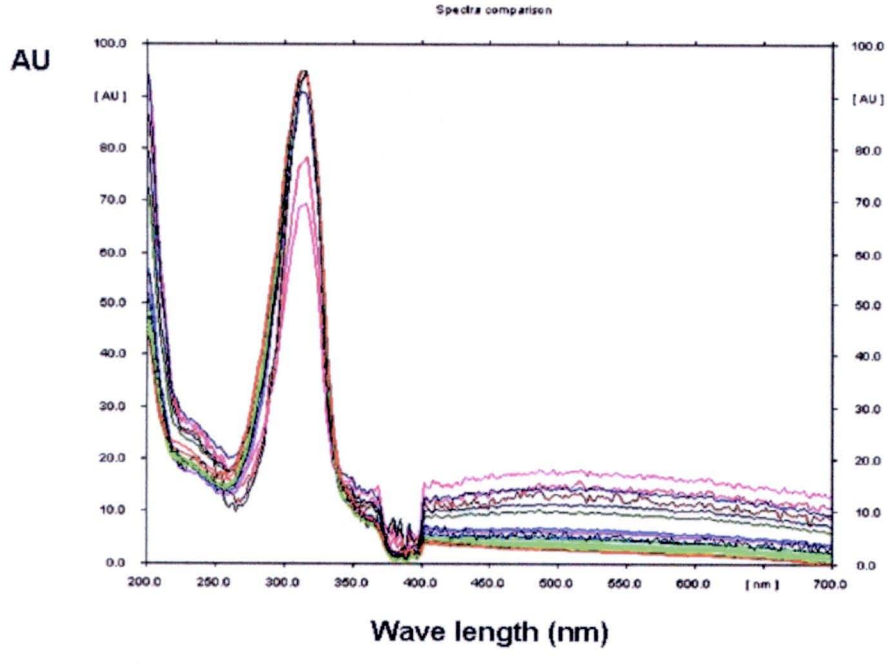

Figure 44 UV-absorption spectra of chromophore obtained from scanning by wavelength on their spots on a silica gel plate of crude extracts prepared from the transgenic and untransgenic plantlets of *A. annua*

The TLC plate was then scanned using TLC-densitometer (CAMAG TLC SCANNER 3, winCATS-Plana Chromatography Manager program, Version 1.4.2.8121, CAMAG, Switzerland) under wavelength of 313 nm.

In terms of the artemisinin content, variation of chemical composition in the hexane extracts was also observed as shown under UV at wave length 366 nm. Figure 42 demonstrats that the TLC pattern of untransgenic and transgenic *A. annua* plantlets before (Figure 42A) and after (Figure 42B) conversion of artemisinin to the chromophore compound (Koobkokkruad et al., 2007). It can be seen that there were differences in both the degree of chemical intensity and chemical profile among the samples. In addition, the artemisinin band intensities were clearly showed that the transgenic *A. annua* higher than untransgenic plantlets.

In addition of the data analysis, the peak area of artemisinin band were analyzed by winCATS-Plana Chromatography Manager program Version : 1.4.2.8121 as show in Figure 43. After being scanned by a TLC-densitometer to obtain the peak area of artemisinin, it was found that symmetry peak at Rf 0.3. For confirmed the artemisinin peak, the band were scanned specific spectrum of this compound. Figure 44 showed the specific spectrum of the artemisinin band. The results indicated that these bands were the artemisinin compound.

The artemisinin contents of the transgenic *A. annua* plantlets were 0.8-1.0 % DW weight more than untransgenic *A. annua* plantlets in range of 0.3-0.4 % DW (Figure 45). These results indicated that transgenic plant of *A. annua* did contain *ads* gene and could express under the expression vector have high enzyme activity of ADS which, in turn, caused the increase in the overall yield of artemisinin in *A. annua* plant.

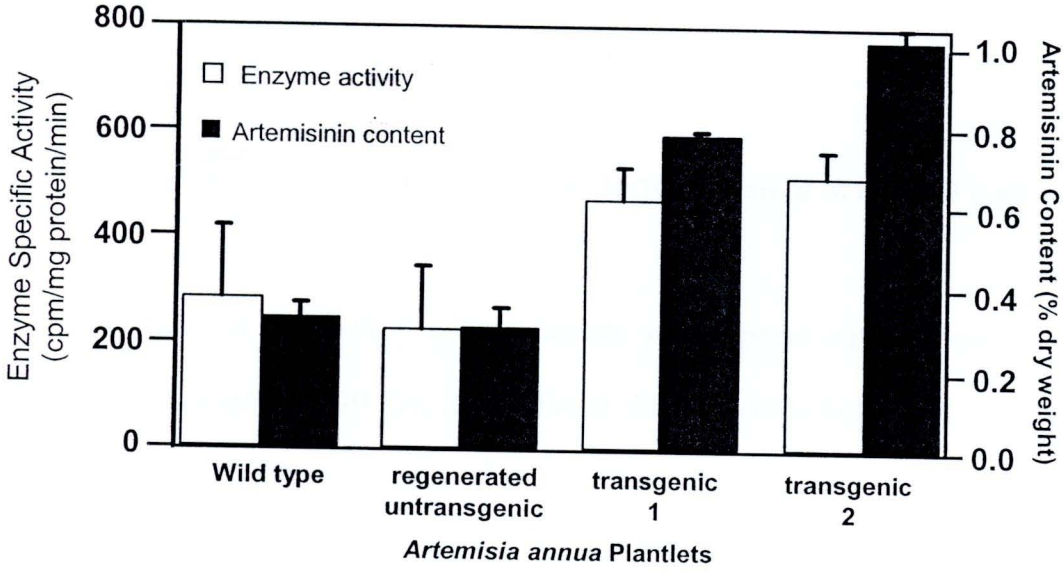

Figure 45 Relationship between amorpha-4,11-diene synthase activity (□) and artemisinin content (■) in wild type, regenerated untransgenic, and transgenic of *A. annua* plantlets